ELSEVIER

Nuclear Instruments and Methods in Physics Research A 494 (2002) 142–147

NUCLEAR INSTRUMENTS & METHODS IN PHYSICS RESEARCH Section A

www.elsevier.com/locate/nima

Micropattern gaseous detectors in the COMPASS tracker ☆

B. Ketzer

CERN, CH-1211 Geneva 23, Switzerland

Abstract

The tracking of particles in the region close to the high-intensity beam of the COMPASS experiment at CERN is based on two novel types of micropattern gaseous detectors, the Micromegas and the GEM. Chosen for their high localization accuracy and rate capability, intrinsic to this technology of highly granular gaseous devices, their large active area of up to 40×40 cm^2 and small material budget offer additional advantages for tracking of particles in a high-luminosity experiment. The basic principles of these detectors as well as the design adopted for the COMPASS experiment, aiming at optimization of operation according to their positions in the spectrometer, are presented. Means to minimize the probability of gas discharges, and to reduce their impact on detector operation, as implemented for both detector types, are discussed. For the 2001 run of COMPASS, over 50% of the total number of detectors required for the full setup was installed and successfully operated. First results concerning the operational characteristics in the COMPASS muon beam are presented.

PACS: 29.40.Cs; 29.40.−n; 29.30.−h

Keywords: Micropattern gaseous detectors; Micromegas; Gas electron multiplier; High-rate tracking; Position-sensitive particle detectors

1. Introduction

The COMPASS experiment at CERN [1] is a new fixed target experiment designed to address a number of physics questions regarding the structure and the spectroscopy of hadrons. This requires the use of high-intensity beams of 2×10^8 muons of 160 GeV/c per 5 s spill, and 10^8 protons, kaons, and pions of 100–280 GeV/c. Its main objective in the first runs is the measurement of the gluon contribution to the nucleon spin in semi-inclusive deep inelastic scattering of polarized muons off polarized nucleons. The production of open charm through photon–gluon fusion ($\gamma g \to c\bar{c}$) is particularly sensitive to the relative orientation of photon and gluon spins. To achieve high mass resolution for charmed D^0 and $\bar{D}^0$ mesons over a wide momentum range, and to maximize angular acceptance, COMPASS was designed as a two-stage magnetic spectrometer, as shown in Fig. 1. The first, large-angle section aims at detecting particles with momenta as low as 0.5 GeV/c, while the second section is optimized for particles with momenta above 10 GeV/c.

The tracking system comprises a set of nested detectors of increasing rate capability, dictated by the increasing particle rates close to the beam axis. The reduced flux in the outermost regions, covered

☆ Invited talk at the 8th International Conference for Colliding Beam Physics (Novosibirsk, 2002).

E-mail address: bernhard.ketzer@cern.ch (B. Ketzer).

0168-9002/02/$ - see front matter
PII: S0168-9002(02)01457-2

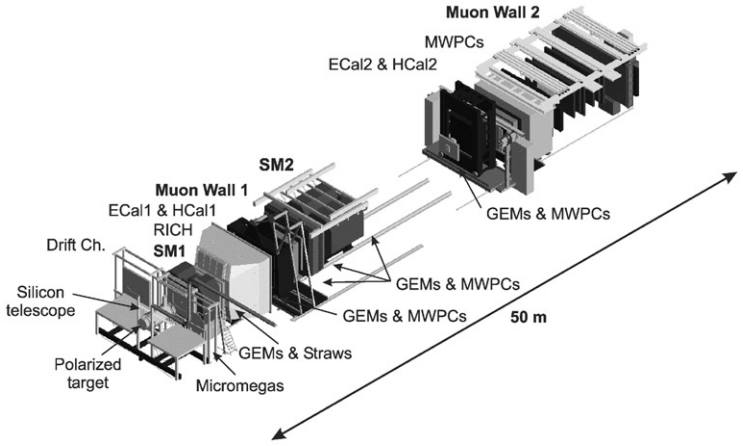

Fig. 1. The COMPASS spectrometer at CERN's SPS accelerator.

by the Large Area Tracker (LAT), allows the use of Multiwire Proportional Counters and several varieties of drift chambers (Drift chambers, Straw tubes, Iarocci tubes). The Very Small Area Trackers cover the beam region up to a radial distance of 2.5–3 cm. Silicon microstrip detectors and scintillating fibers fulfill this task. The intermediate region at a radial distance of 2.5 to 30–40 cm is covered by the Small Area Trackers (SAT), and is the domain of micropattern gas detectors. In front of the first spectrometer magnet, the full setup comprises three stations of Micromegas, each made of 4 planes measuring the horizontal (X) and vertical (Y) projections, and two projections inclined by $\pm 45^\circ$ (U, V). Downstream of the magnet, the Small Area Tracking is performed by 10 GEM stations, each made of two GEM detectors measuring projections XY, and UV, respectively.

The particle rates the tracking detectors have to cope with not only depend on the radial distance from the beam, but also on the longitudinal position along the beam direction. Here, the most stringent requirements concern the section upstream of the first spectrometer magnet, where the detectors are traversed by the full spectrum of particles produced in the target, the low-energy background not having been swept away by the analyzing magnet. Similar rates are expected for the most downstream detectors, where the divergence of the muon beam causes a significant

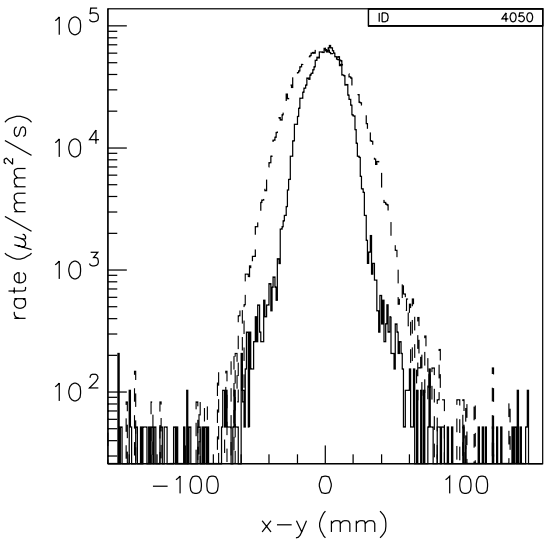

Fig. 2. Rate of muons for two orthogonal cross-sections through the beam center at a longitudinal position of ~ 10 m downstream of the target.

fraction of the beam halo to be seen by the detectors outside their inactive central region of 5 cm diameter. Fig. 2 shows the rate of muons at a longitudinal position of ~ 10 m downstream of the target, for two orthogonal cross-sections through the beam center. Obviously, the detectors in the SAT have to be able to withstand particle rates of more than 1 MHz/cm^2 at a distance of 2.5 cm to the beam axis. For a typical strip pitch

of 400 μm, this transforms into a projected rate of ~100 kHz/strip. Fast removal of slow ions and high granularity are essential to achieve such high rate capabilities.

In addition to these constraints concerning rate capability, the physics program also sets requirements on the spatial resolution of the detectors, which should be considerably better than 100 μm. To achieve the required mass resolution for D^0 mesons of 10 MeV, multiple scattering in the tracking detectors has to be kept at a minimum, with one detector plane accounting for less than 0.5% of a radiation length. Needless to say that the performance of the detectors must not deteriorate under sustained irradiation (''aging'') or due to gas discharges.

2. The Micromegas detectors

The Micromegas (**Microme**sh **Ga**seous **S**tructure) [2] is a two-stage parallel plate electrode gas detector, where a low-field, 3.2 mm thick conversion/drift space is separated from a 100 μm thick, high-field amplification gap by a thin metal grid (micromesh), as shown schematically in Fig. 3. Primary electrons created in the conversion gap drift into the amplification region where a high electric field of ~50 kV/cm initiates an avalanche. While electrons drift towards the readout structure, a set of parallel microstrips with 360 μm pitch in the central part and 420 μm in the outer region, positive ions created in the thin gap are quickly evacuated on the grid, giving rise to the required rate capability of the detector. The drift mesh and the micromesh are both made of 4 μm thick nickel grids with a density of 200 and 500 lines per inch, respectively. The distance between the micromesh and the anode strips is defined by cylindrical spacers of 150 μm diameter, which are made of etchable resin and are an integral part of the readout structure, manufactured in a technology very similar to the GEM fabrication. The detectors built for COMPASS have a large active area of $40 \times 40\ cm^2$ with a central dead area of 5 cm diameter. The readout strips extend over 35 cm outside the active area, allowing the front-end electronics to be mounted outside the acceptance of the spectrometer [3].

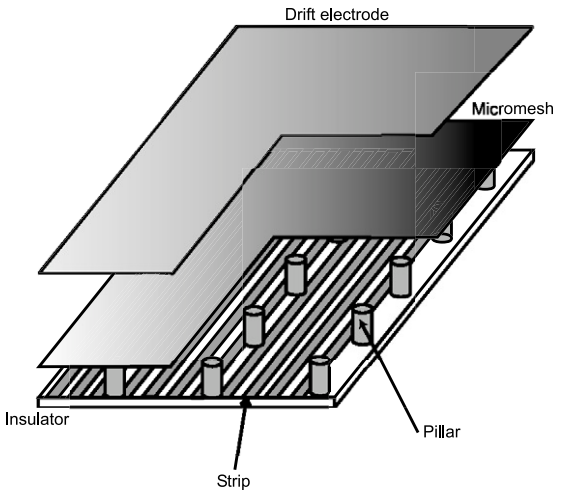

Fig. 3. Schematic view of a Micromegas detector.

The detectors are operated in a gas mixture of $Ne–C_2H_6–CF_4$ (80–10–10), which was found to compare favourable to Ar-based mixtures in terms of spatial and time resolution. In addition, the probability of a gas discharge upon exposure of the detector to ionizing tracks, a phenomenon common to all micropattern gas detectors, is reduced for this gas. A discharge rate of less than 0.1/spill was observed in the high-intensity muon beam of COMPASS. To reduce the total charge released to the front-end electronics in a discharge, a 100 pF decoupling capacitor was introduced for each strip. This capacitor allows the potential of the strips involved in the discharge to vary much faster than the potential of the mesh, thus limiting the resulting large gain drop to the region of the discharge [3].

In order to achieve a time resolution compatible with the large particle flux expected in front of the first spectrometer magnet, a digital read-out of both the leading and trailing edges of the signal from the detector is employed, using a 16-channel amplifier discriminator chip (SFE16) in combination with a multi-hit TDC (F1). From the mean value of leading and trailing edges and from the time over threshold both the time of the signal and its amplitude can be deduced.

3. The GEM detector

The **G**as **E**lectron **M**ultiplier (GEM) [4] consists of a 50 μm thin insulator foil, metallized on both surfaces, into which a large number of microscopic holes (70 μm diameter at a distance of 140 μm) is chemically etched. Inserting the foil in the gas volume between a drift cathode and a read-out anode, and applying a suitable potential between the two sides, electrons created by ionizing radiation in the drift gap drift into the holes, are multiplied due to the high electric field, and released to the other side, where they can be collected or further amplified. Ions are created in the holes only, and are quickly evacuated, so that the signal on the read-out structure is entirely due to electron collection, and hence intrinsically fast.

The COMPASS GEM detectors consist of three cascaded GEM amplification stages, with a conversion/drift gap of 3 mm, and gaps between GEM foils and to the read-out anode of 2 mm, the distances between electrodes being guaranteed by grids of thin fiberglass strips. Fig. 4 shows an exploded view of the detector [5]. Sharing the total gain necessary for efficient detection of minimum ionizing particles between three amplification stages, with the gain gradually decreasing by

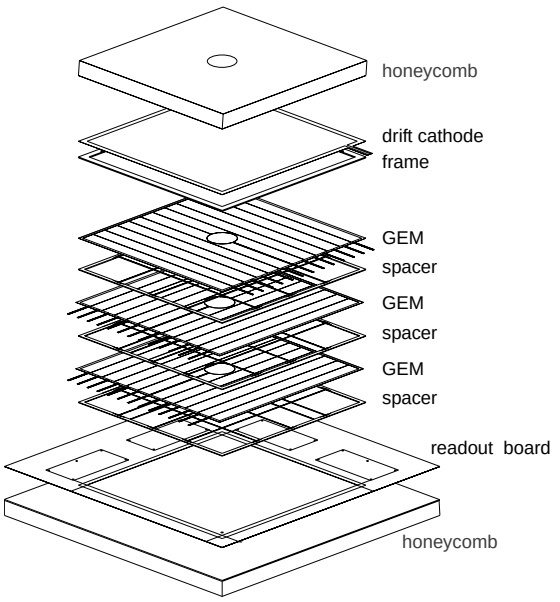

Fig. 4. Exploded view of a COMPASS GEM detector.

$\sim 20\%$ from the first to the third GEM, reduces the probability of a discharge triggered by heavily ionizing particles by more than two orders of magnitude with respect to a double GEM structure with equal gain sharing. In addition, the energy stored in each GEM foil is decreased by subdividing it into individually powered sectors. This way, both the charge released in a discharge is decreased, and the probability that a discharge that started between the two GEM electrodes propagates to the anodes is minimized [6]. The central region of the detector, traversed by the high-intensity beam, is deactivated during normal operation by decreasing the potential of a disk-shaped sector in the center of the third GEM foil. Restoring the nominal potential by a simple switch, however, the center can be activated, a feature of great importance for alignment purposes using a low-intensity beam. Owing to the clear separation of amplification and read-out stages, a feature unique to purely GEM-based detectors, a two-dimensional projective read-out of the signals is accomplished, making use of a printed circuit board with two layers of orthogonal strips, insulated by thin ridges of 50 μm Kapton. The widths of strips were adjusted so that each layer collects about half of the total charge in the avalanche. The COMPASS GEM detectors operate in $Ar–CO_2$ (70–30), a mixture which was chosen due to its favourable properties as non-flammability, low diffusion and large drift velocity of electrons, and non-polymerization.

The read-out electronics makes use of an analogue sampling at 40 MHz of the amplified and shaped signal on each input strip by the APV25 chip. The sampled amplitudes are then stored in a pipeline, allowing for a maximum delay of 4 μs until the trigger decision is taken. Upon arrival of a trigger, the amplitudes in 3 consecutive samples of each channel are multiplexed and digitized by an ADC, which also performs zero suppression to reduce the data rate.

4. Performance in particle beams

For the 2001 run of COMPASS, 6 out of 12 Micromegas detectors and 14 out of 20 GEM

detectors equipped with final front-end electronics were installed and operated. Here we report preliminary results obtained during the commissioning phase of these detectors at moderate beam intensities of $\sim 10^7$ μ/spill. Straight line tracking was performed using other Micromegas or GEM detectors close to the detector under investigation.

Fig. 5(a) shows the efficiency for the detection of minimum ionizing particles in one COMPASS Micromegas plane as a function of the mesh voltage. The plateau of ~98% is reached at a voltage of 410 V, corresponding to a gain of 6400. The corresponding time resolution is displayed in Fig. 5(b). A value of ~10 ns is reached at the beginning of the efficiency plateau.

For the COMPASS GEM detectors, full detection efficiency for both projections is reached at a gain of 8000 V. The fact that the total charge is shared equally by the two read-out coordinates is illustrated in Fig. 6, where the cluster amplitude recorded for each event on one projection is plotted versus the amplitude on the second projection [6]. The narrow correlation with a ratio of ~1 and a sigma of ~0.1 will be exploited to resolve ambiguities in the case of multi-hit events. The spatial resolution of the GEM detectors can be deduced from the distribution of hit-residuals relative to the predicted position, shown in Fig. 7, by deconvoluting uncertainties in the tracking and effects of multiple scattering, and is calculated to be ~50 μm.

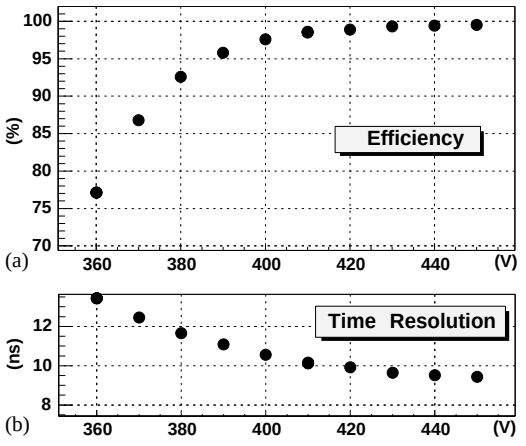

Fig. 5. Efficiency (a) and time resolution (b) of the COMPASS Micromegas detector, as a function of the potential applied to the micromesh.

5. Summary and outlook

With two novel types of large-size detectors, Micromegas and GEMs, successfully operating in a high-rate experiment like COMPASS, micropattern gaseous detectors have reached maturity. They prove to withstand high particle rates, and cover relatively large areas, and at the same time maintain a spatial resolution far better than 100 μm.

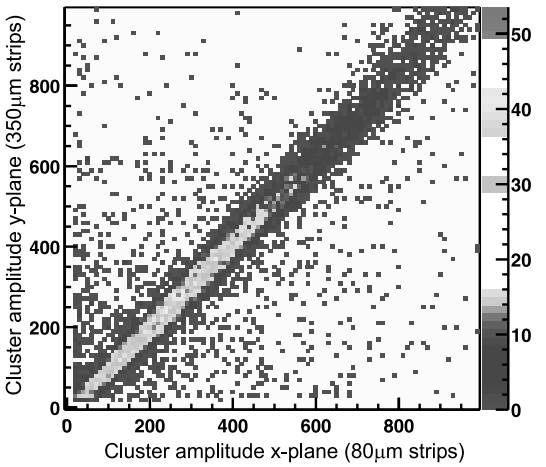

Fig. 6. Correlation of cluster amplitudes recorded on the upper (80 μm width) and lower (350 μm width) layer of GEM read-out strips.

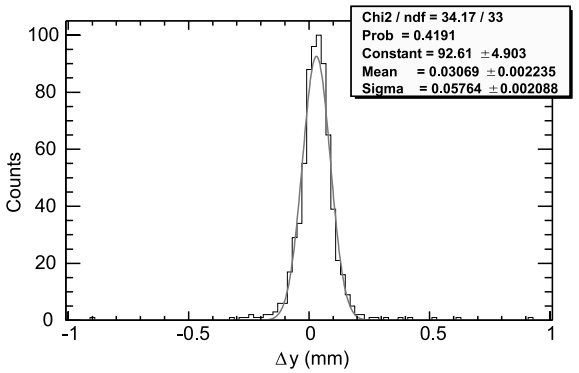

Fig. 7. Distribution of hit-residuals from the predicted track position.

Due to their position in front of the first spectrometer magnet, Micromegas are subject to very high particle fluxes, which required optimization of their time resolution to reduce the number of accidental hits. Employing a custom-made read-out, a time resolution around 10 ns was reached. The GEM detectors, performing the small area tracking downstream of the first spectrometer magnet, were built using as little material as possible, with one detector measuring the traversing particles in two projections, while accounting only for about 0.4% of a radiation length on the beam axis, and for 0.7% in the active area. In addition, the two-dimensional read-out gives rise to a very good multi-hit resolution of the GEM detectors.

The problem of discharges, origin of continuing problems with first generation micropattern gas detectors like MSGCs in high-rate experiments, seems to be well under control. After extensive R& D on discharge phenomena, strategies were found to prevent to a large extent the occurrence of gas breakdowns, e.g. multi-stage amplification in the case of GEMs, or optimization of field configurations and gas mixtures. Where they cannot be completely avoided, their impact on detector performance has to be minimized, as successfully shown for the Micromegas, where the dead time after a discharge has been reduced to some ms, and the front-end electronics is fully protected against overcurrents.

For the 2002 run of COMPASS, the remaining six planes of Micromegas and six double planes of GEM detectors have been installed and are being commissioned. With a total number of almost 50,000 read-out channels for the Small Area Tracker fully operational, there are good prospects for first physics results from COMPASS.

References

[1] The COMPASS Collaboration, COMPASS: a proposal for a common muon and proton apparatus for structure and spectroscopy, CERN/SPSLC 96-14, SPSC/P 297, March 1996.

[2] Y. Giomataris, P. Rebourgeard, J.P. Robert, G. Charpak, Nucl. Instr. and Meth. A 376 (1996) 29.

[3] D. Thers, P. Abbon, J. Ball, Y. Bedfer, C. Bernet, C. Carasco, E. Delagnes, D. Durand, J. Faivre, H. Fonvieille, A. Giganon, F. Kunne, J.L. Goff, F. Lehar, A. Magnon, D. Neyret, E. Pasquetto, H. Pereira, S. Platchkov, E. Poisson, P. Rebourgeard, Nucl. Instr. and Meth. A 469 (2001) 133.

[4] F. Sauli, Nucl. Instrum. and Meth. A 386 (1997) 531.

[5] C. Altunbas, M. Capeáns, K. Dehmelt, J. Ehlers, J. Friedrich, I. Konorov, A. Gandi, S. Kappler, B. Ketzer, R.D. Oliveira, S. Paul, A. Placci, L. Ropelewski, F. Sauli, F. Simon, M. van Stenis, Construction, test and commissioning of the triple-GEM tracking detectors for COMPASS, Nucl. Instr. and Meth. A 490 (2002) 177.

[6] B. Ketzer, M. Altunbas, K. Dehmelt, J. Ehlers, J. Friedrich, B. Grube, S. Kappler, I. Konorov, S. Paul, A. Placci, L. Ropelewski, F. Sauli, F. Simon, Triple GEM tracking detectors for COMPASS, IEEE Trans. Nucl. Sci. 49 (Oct.) (2002) in press (Preprint CERN-OPEN-2002-004).